

# Design of tunable power detector towards 5G applications

Issa Alaji<sup>1</sup>, Walid Aouimeur<sup>2</sup>, Haitham Ghanem<sup>1</sup>, Etienne Okada<sup>1</sup>, Sylvie Lépilliet<sup>1</sup>,  
Daniel Gloria<sup>3</sup>, Guillaume Ducournau<sup>1</sup> and Christophe Gaquière<sup>1</sup>

<sup>1</sup> IEMN, Avenue Henri Poincaré, cité scientifique CS 60069, VILLENEUVE D'ASCQ, 59652, France

<sup>b</sup> TiHIVE, 29 chemin du vieux chêne, Meylan, 38240, France

<sup>3</sup> STMicroelectronics, 850 rue Jean Monnet, Crolles, 38920, France

---

## Abstract

This paper presents the design and characterization of two tunable power detectors, based on PN diodes, integrated in SiGe 55-nm BiCMOS technology from ST-Microelectronics. The working frequency band of the circuits is (35-50) GHz dedicated for 5G applications. The detector parameters are adjusted by controlling the biasing current, this characteristic makes them suitable to be utilized in different 5G applications. Two different diode sizes are used (L1N1, L2N5) in order to compare their performances. For three values of biasing current, the extracted voltage sensitivity values are between (700 - 1400) V/W for L1N1 and (500 - 1150) V/W for L2N5 showing the agreement with the simulation. Comparing to recent works, our designs exhibit very low power consumption (down to 60 nW) with relatively high sensitivity values. A targeted sensitivity value can be obtained with lower power consumption using larger diode size.

*Keywords:* 5G and IoT sensors, 55-nm BiCMOS, tunable power detector, Millimeter wave, PN diode.

---

## 1. Introduction

The interest of 5G and its relation to the IoT (Internet of Things) have been growing rapidly since its initial launch in 2012 [1]. The IoT sensors will be located everywhere (car, home, industrial health monitoring, etc.) providing increased machine-to-machine connectivity [2]. With the diversity of the applications provided by 5G and IoT systems, power detectors with different characteristics are required following the applications. In this context, we present the design and characterization of two adjustable (tunable) power detectors, based on PN diodes, integrated in the 55-nm SiGe BiCMOS technology from ST- Microelectronics. The working frequency band is (35 - 50) GHz allowing the detectors to cover several 5G bands (37 - 40.5) GHz, (42.5 - 43.5) GHz, (45.5 - 47) GHz and (47.2 - 50.2) GHz [3]. When the value of biasing current is adjusted, all the detector parameters can be tuned. This includes the video resistance, maximum input RF power ( $P_{in,max}$ ), voltage sensitivity, and power consumption. This characteristic makes the detectors usable in different 5G applications providing adjustable parameters.

## 2. Detector Design

Two power detectors are designed based on two sizes of PN diodes (named as L1N1 and L2N5), hence, we will name the detector by the diode name. The L1N1 and L2N5 correspond to diode sizes of 0.34 and 3.4  $\mu\text{m}^2$  respectively. The objectives are to: (i) design a tunable power detector, suitable for different 5G applications, (ii) investigate the effect of the diode size on the detectors

---

Corresponding author:

email address: issa.alaji.etu@univ-lille.fr

performance. The block diagram of the detector circuit is shown in Figure 1. In the following sections, each block circuit is discussed, then, the simulation of the detectors using ADS Keysight© software is explained.

[Figure 1]

### 2.1 N-load circuit

The N-load circuit consists of NMOS transistor with stub network. This circuit absorbs (thus attenuate) a part of the input RF power. Attenuating the input power allows to maintain the linearity of the detector at higher level of input power ( $P_{in} > -30$  dBm). However, it decreases the sensitivity value. Hence, the best trade-off between the sensitivity and linearity has to be considered.

Using Cadence virtuoso software (which provides the design kit of the technology), the NMOS transistor and stubs are sized to exhibit about  $40 \Omega$  as real impedance ( $\text{real}(Z_{load})$ ) in the frequency bandwidth (35 – 50) GHz. No power is consumed in the N-load circuit because of two reasons: (i) it exhibits a short circuit at DC, (ii) the NMOS transistor is driven through its gate by a certain DC voltage (0.53 V).

### 2.2 Extraction of the diode parameters

The small signal model of the diode was extracted up to 110 GHz [4] and is shown in Figure 2. The  $R_j$  and  $C_j$  represent the resistance and capacitance of the junction,  $R_s$  represents the equivalent series resistance, and  $C_p$  represents the capacitance of the back-end structure. The substrate effects represented by  $R_{sub}$ ,  $C_{sub}$ ,  $C_{ox}$  are negligible up to 110 GHz [4]. In order to use the diodes in simulation, different diode parameters are extracted. The elements values of the diodes model (of L1N1 and L2N5) were extracted for three biasing currents (0.1, 1, 10)  $\mu\text{A}$  using the same method proposed in [4].

[Figure 2]

The diode I-V characteristic is given as in [5]:

$$I = I_s \cdot (\exp(V / n \cdot V_T) - 1) \quad (1)$$

Where  $I$ , and  $V$  are the current and voltage across the junction,  $n$  is the ideality factor,  $I_s$  is the saturation current, and  $V_T$  is the thermal voltage. The I-V curves of L1N1 and L2N5 were measured and used to extract the  $n$  and  $I_s$  values as in [6].

### 2.3 Matching network

The matching network is important to ensure that the maximum RF power is absorbed by the detector, meanwhile avoiding standing waves. In order to design the matching network, the diode with the N-load circuit are simulated in Cadence virtuoso for two detectors (L1N1 and L2N5), where the diodes are represented by their extracted small signal models.

It is worth to mention that, the matching networks are designed for wide range of biasing current value (1 nA - 100  $\mu\text{A}$ ) enabling the tuning of detectors parameters.

## 2.4 Detection simulation in ADS

The large signal model of the diode is required for detection simulation. The Symbolically Defined Devices (SDD) box available in ADS software is suitable to represent the nonlinear behavior of  $R_j$ . Therefore, ADS is chosen (instead of Cadence virtuoso) for detection simulation. The SDD box is defined by Eq. (1) where the extracted  $n$  and  $I_s$  values are provided. The 50 fF capacitor ( $C_m$ ) is connected in parallel with the diode in order to help to match the detector for wider range of biasing currents  $I_b$ . This capacitance is assumed to be dominant comparing to the variation of the  $C_j$  values with input RF power. This assumptions will be validated by comparing the simulated to measured results. Based on the assumption above, the extracted  $C_j$  values (from the linear model) are used in the large signal model of the diodes.

The complete circuits of the detectors are simulated in ADS, where the matching networks and N-load circuit are represented by their extracted equivalent circuits from Cadence virtuoso, the diodes are represented by their large signal models. Harmonic balance simulation is used to simulate the output DC voltage  $V_{out}$  when the input RF power is applied. In addition, matching the detectors for large signal input power (up to  $-10$  dBm) is also verified using large signal S-parameter simulation (LSSP).

## 3. Measurement Results

### 3.1 Voltage sensitivity definition

When the detector is biased by a DC current ( $I_b$ ), we define the DC output voltages ( $V_{OFF}$ ) and ( $V_{ON}$ ) when the input RF power is in the states (OFF) and (ON) respectively. The voltage sensitivity (response coefficient in V/W) of the detector is given as:

$$\gamma = \frac{V_{OFF} - V_{ON}}{P_{in}} \quad (2)$$

In Eq. (2),  $P_{in}$  is the available power at the input pad plane.

### 3.2 Measurement of the reflection coefficient

Figure 3 shows the measured and simulated  $S_{11}$  curves of the detectors L1N1 and L2N5. These curves are shown for three values of biasing current  $I_b$ . It can be noticed that the detectors L1N1 and L2N5 are matched in the frequency bands (35-50) GHz and (35-48) GHz respectively, where  $|S_{11}| \leq -8$  dB.

[Figure 3]

### 3.3 Measurement of the voltage sensitivity

The bench setup used to extract the voltage sensitivity is shown in Figure 4. A coplanar probe Infinity i67 is used at the input (RF side), and a high impedance Cascade Microtech

probe FPX-100X at the output (DC side).

[Figure 4]

A KEITHLEY-2440 DC source meter is used as a current source to bias the detector. In order to measure the DC output voltage ( $V_{out}$ ), a DC voltmeter Agilent-34461A is used providing higher measurement accuracy than the source meter. Both the source meter and voltmeter have internal impedance about 10 G $\Omega$ . DC voltage source is used to drive the N-load circuit through DC needles. The RF power is injected using PSG (Performance Source Generator E8257D) in the frequency band (35-50) GHz, where the input RF power  $P_{in}$  is defined at the input pad plane as shown in Figure 4. To extract the voltage sensitivity values, the values of ( $V_{OFF}$ ) and ( $V_{ON}$ ) are measured and then applied in Eq. (2).

Based on Figure 5 (a, b), it can be concluded that: (i) the sensitivity curves are relatively flat in the frequency band of interest, (ii) a good agreement is obtained between the simulation and measurement results, (iii) the higher the biasing current, the lower is the sensitivity value.

Based on Figure 5 (c, d), it can be concluded that: (i) the lower the sensitivity value, the higher is the compression point  $P_{in,max}$ . The  $P_{in,max}$  points corresponding to biasing currents (0.1, 1, 10)  $\mu$ A occur at (-20, -18.7, -12) dBm for L1N1, and (-18, -16, -8) dBm for L2N5 respectively, (ii) a good agreement is obtained between the simulation and measurement results.

[Figure 5]

Since the DC power is only consumed in the diodes, the power consumptions ( $P_D$ ) of the detectors are calculated using the measured I-V characteristics as in Eq. (3).

$$P_D = V_{OFF} \times I_b \quad (3)$$

The video resistance values  $R_v$  of the detectors are equal to the extracted  $R_j$  values and inversely proportional to the biasing current.

The comparison with other recent works is presented in Table 1, our designs performances are beyond the current state of the art exhibiting very low power consumption with relatively high sensitivity values.

[Table 1]

Based on the results of this work, it can be concluded that a targeted sensitivity value with lower power consumption can be obtained using a larger diode, as it is the case for (detector L1N1 biased with  $I_b = 1 \mu$ A) and (detector L2N5 biased with  $I_b = 0.1 \mu$ A). However, the larger diode exhibits higher video resistance reducing the video bandwidth ( $R_v = 25$  and  $250$  k $\Omega$  for L1N1 and L2N5 respectively).

The  $S_{11}$  measurements show that the detectors are matched when the current  $I_b$  is in the range (1 nA - 100  $\mu$ A), providing (simulated) sensitivity values (10 - 1500) V/W for the detector L1N1. However, those values were not extracted due to the accuracy limitation of the source meter and voltmeter.

#### 4. Conclusion

The synthesis and characterization of two tunable power detectors dedicated for 5G applications were presented, where each detector is based on different size of PN diode. N-load circuit was designed to help maintaining the linearity at higher input powers without increasing the DC power consumption. Adjustable value of voltage sensitivity is obtained

(700 - 1400) V/W for the detector L1N1, and (500 - 1150) V/W for the detector L2N5 . The detector with larger diode requires lower power consumption to achieve a certain sensitivity value, however, it exhibits higher video resistance.

## Acknowledgments

This research work is carried in the framework of the 16ENG06 ADVENT project which is supported by the European Metrology Program for Innovation and Research (EMPIR).

## References

- [1] Chen, S., Kang, S. A tutorial on 5G and the progress in China. *Frontiers Inf Technol Electronic Eng* 19, 309–321 (2018). <https://doi.org/10.1631/FITEE.1800070>
- [2] J. M. Khurpade, D. Rao and P. D. Sanghavi, "A Survey on IOT and 5G Network," 2018 International Conference on Smart City and Emerging Technology (ICSCET), Mumbai, 2018, pp. 1-3.
- [3] Sgora, Aggeliki. (2018). 5G Spectrum and Regulatory Policy in Europe: An Overview. 1-5. 10.1109/GIIS.2018.8635764.
- [4] J. Goncalves, I. Alaji, D. Gloria, V. Gidel, F. Gianesello, S. Lepilliet, G. Ducournau, F. Danneville, and C. Gaquière; «On Wafer Millimetre Wave Power Detection Using a PN Junction Diode in BiCMOS 55 nm for In-Situ Large Signal Characterization» EUROPEAN MICROWAVE WEEK 2018.
- [5] C. Sah, R. N. Noyce and W. Shockley, "Carrier Generation and Recombination in P-N Junctions and P-N Junction Characteristics," in *Proceedings of the IRE*, vol. 45, no. 9, pp. 1228-1243, Sept. 1957.
- [6] Gül, Fatih. (2019). Addressing the sneak-path problem in crossbar RRAM devices using memristor-based one Schottky diode-one resistor array. *Results in Physics*. 12. 1091-1096. 10.1016/j.rinp.2018.12.092.
- [7] C. Li, X. Yi, C. C. Boon and K. Yang, "A 34-dB Dynamic Range 0.7-mW Compact Switched-Capacitor Power Detector in 65-nm CMOS," in *IEEE Transactions on Power Electronics*, vol. 34, no. 10, pp. 9365-9368, Oct. 2019.
- [8] M. Saeed et al., "0.15 mm<sup>2</sup>, DC-70GHz, Graphene-Based Power Detector with Improved Sensitivity and Dynamic Range," 2018 IEEE/MTT-S International Microwave Symposium - IMS, Philadelphia, PA, 2018, pp. 1519-1522.
- [9] M. Hrobak, M. Sterns, M. Schramm, W. Stein and L. Schmidt, "Planar zero bias schottky diode detector operating in the E- and W-band," 2013 European Microwave Conference, Nuremberg, 2013, pp. 179-182.
- [10] S. Qayyum and R. Negra, "0.8 mW, 0.1–110 GHz RF power detector with 6 GHz video bandwidth for

multigigabit software defined radios," 2017 IEEE MTT-S International Microwave Symposium (IMS), Honolulu, HI, 2017, pp. 1722-1725.

- [11] A. Serhan, E. Lauga-Larroze and J. Fournier, "A 700MHz output bandwidth, 30dB dynamic range, common-base mm-wave power detector," 2015 IEEE MTT-S International Microwave Symposium, Phoenix, AZ, 2015, pp. 1-3.

## Figures and Tables

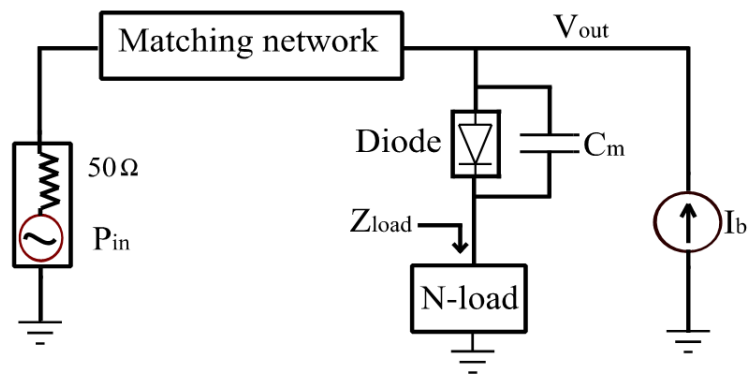


Figure 1 Block diagram of the detector circuit.

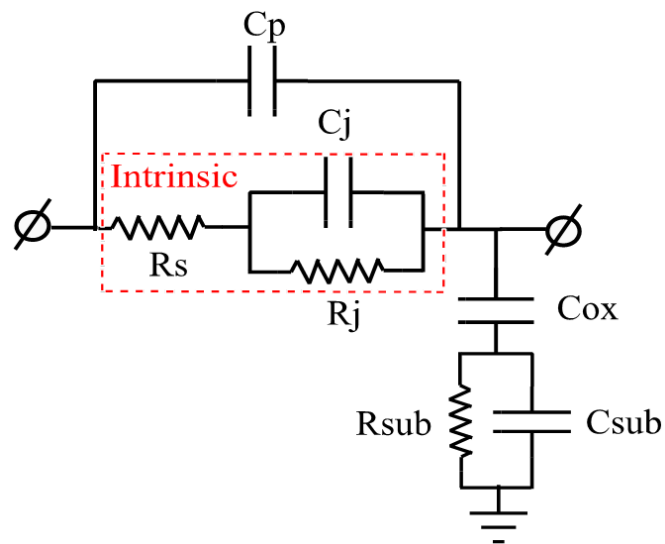


Figure 2 The small signal model of the PN diode.

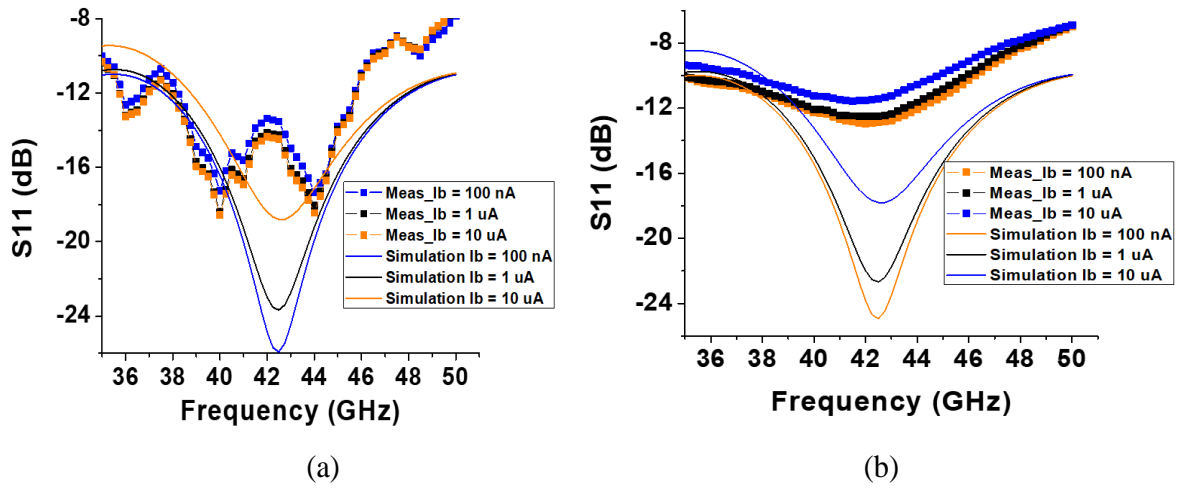


Figure 3 The measured and simulated  $S_{11}$  for: (a) L1N1, (b) L2N5 detectors at  $P_{in} = -12$  dBm.

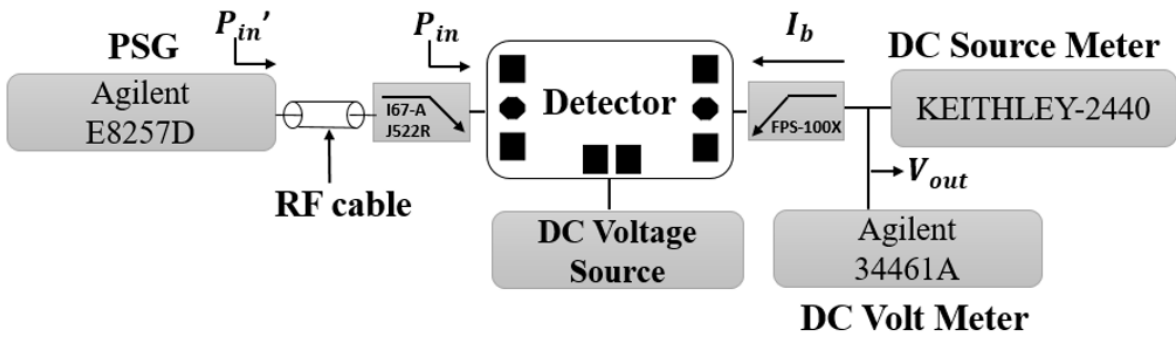
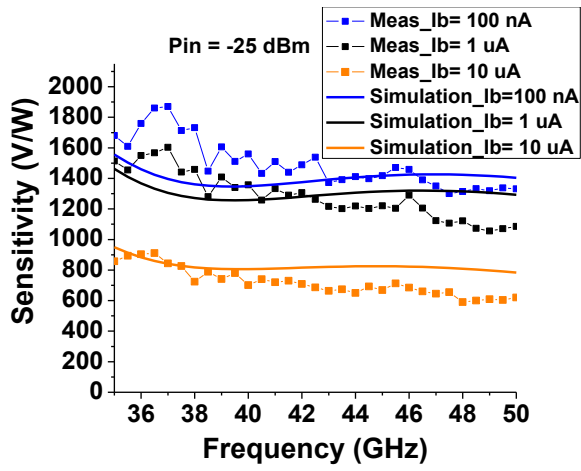
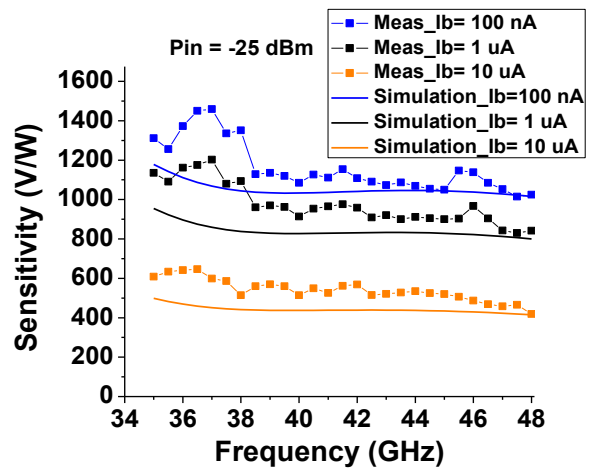


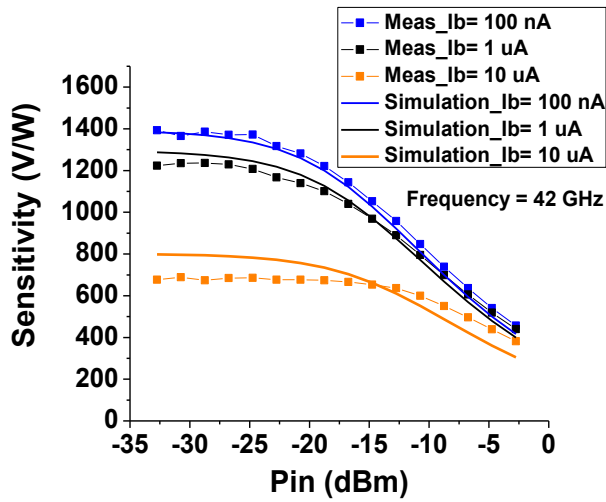
Figure 4 Test bench block diagram to extract the voltage sensitivity value.



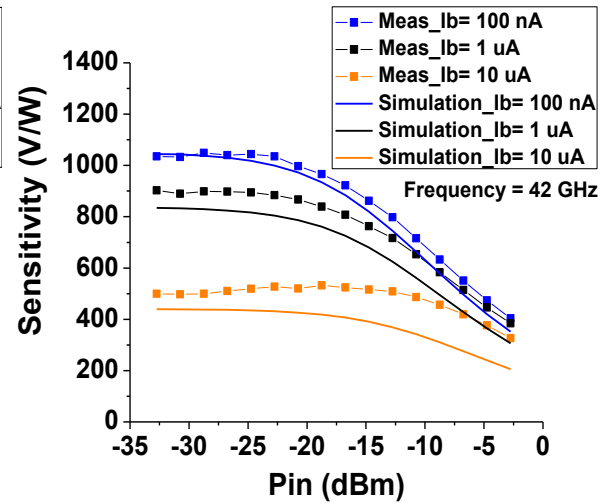
(a)



(b)



(c)



(d)

Figure 5 The measured and simulated voltage sensitivity curves vs: (a) frequency for L1N1, (b) frequency for L2N5, (c) input power for L1N1, (d) input power for L2N5.



Table 1 Comparison with other published power detectors.

Reference	Technology	Frequency (GHz)	Sensitivity (V/W)	$P_D$ ( $\mu$ W)
7	65nm-CMOS PN diodes	4-6	3	700
8	Custom MMIC	0 – 70	87 - 148	0
9	GaAs Shottky diode	60 – 110	2000 - 6000	0
10	65nm-CMOS	0.1 – 110	69 - 125	800
11	55nm-BiCMOS	50 - 66	1500	80
This work	55nm-BiCMOS PN diode	35-50 For L1N1	700 ( $I_b = 10 \mu A$ and $R_v = 2.5 k\Omega$ )	8.3
			1200 ( $I_b = 1 \mu A$ and $R_v = 25 k\Omega$ )	0.77
			1400 ( $I_b = 0.1 \mu A$ and $R_v = 250 k\Omega$ )	0.07
		35-48 For L2N5	500 ( $I_b = 10 \mu A$ and $R_v = 2.5 k\Omega$ )	7.6
			900 ( $I_b = 1 \mu A$ and $R_v = 24 k\Omega$ )	0.69
			1150 ( $I_b = 0.1 \mu A$ and $R_v = 245 k\Omega$ )	0.06